Journal of Mathematical Sciences and Modelling, 5 (1) (2022) 1-7
Research Article

Journal of Mathematical Sciences and Modelling

Journal Homepage: www.dergipark.gov.tr/jmsm
ISSN 2636-8692
DOI: http://dx.doi.org/10.33187/jmsm.1063954

A Mathematical Modelling Approach for a Past-Dependent Prey-Predator System

Aytül Gökçe[1]

[1] *Department of Mathematics, Faculty of Science and Arts, Ordu University, Ordu, Turkey*

Article Info

Keywords: *Nonlinear dynamics, Prey-predator systems, Stability.*
2010 AMS: *34A34, 34DXX, 37C75.*
Received: *27 January 2022*
Accepted: *6 March 2022*
Available online: *30 April 2022*

Abstract

A memory dependent prey-predator model incorporating Allee effect in prey is analysed. For a small and high values of memory rate, the dynamical changes in the prey and predator densities are demonstrated. The equilibria of the proposed model and the local stability analysis corresponding to each equilibrium are presented. The variables of prey and predator species with respect to memory rate are investigated and the existence of the Hopf bifurcation is shown. The analytical part of this paper is supported with detailed numerical simulations.

1. Backround

Mathematical modelling of complex interactions among species through the systems of ordinary differential equations has attracted a great attention by many researchers in the last few decades. These models trace their roots back to a seminal work of Lotka and Volterra and since then numerous papers have been published with various functional responses [1, 2, 3]. The functional response refers to the intake rate of a predator as a function of prey density. The most common functional responses are known as Holling type I-IV functional responses, where type I is the most simplest linear functional form and type II is the most frequently used functional form [4, 5]. Here consumed rate of prey monotonically decrease with its density. Type III response is rather similar to type II in terms of saturation at high prey density, yet a super-linear increase can be observed at lower densities. Apart from these functional forms, some specific interaction functions have been also studied. These include Beddington–DeAngelis interaction functional, Hassel–Varley interaction functional and Ratio-dependent interaction functional [6]. Here we concentrate on Holling type III functional response [7].

There are many social and characteristic factors that affect the interactions of species. Among these, Allee effect and intrascpecific competition have been thoroughly investigated. Allee effect was introduced by Allee to model different circumstances associated with aggregation and related cooperative characteristics [8]. This has been found particularly important to understand the relationship between species' suvival probability and population size [8, 9]. On the other hand, population dynamics may also be influenced by the intraspecific competition in real world scenario [10, 11, 12]. In fact, the resource for survival of species are always limited and thus competition among species of a population is more likely to occur. In this paper we will consider Allee effect in prey population and intraspecific competition in predator population.

In many models of ecology, it is usually assumed that the growth rate of both prey and predator species is respectively associated with the predator and prey density in the present time. However, there has been a great interest in the role of memory in population dynamics, through considering nonlocal addition of past influence or using fractional differential equations. In reality, the predator density not only depends on the current density of prey but also depends on the past density of prey [5, 13, 14]. One way to incorporate memory through ordinary differential equation is to turn a non-local memory function into another differential equation. In this context, an exponential probability density function will be considered.

This paper is organised as in the following order. Firstly, in Sec. 2, the mathematical model is described. The dimensionless version of the proposed model and its steady states are respectively presented in Sec. 2.1 and Sec. 2.2. The local stability analysis for each steady state is given in Sec. 3. Theoretical work presented in these sections will be supported with extensive numerical simulations.

***Email address and ORCID number*: aytulgokce@odu.edu.tr, 0000-0003-1421-3966, (A. Gökçe)**

2. Mathematical Model

The model with memory effects that we will consider in this paper can be written as

$$\begin{aligned}
\frac{\mathrm{d}P}{\mathrm{d}T} &= \alpha P(T)\left(1-\frac{P(T)}{K}\right)(P(T)-\kappa)-\frac{\mu P(T)^2 Q(T)}{\beta+P(T)^2},\\
\frac{\mathrm{d}Q}{\mathrm{d}T} &= \frac{\nu\mu M(T)^2 Q(T)}{\beta+M(T)^2}-\eta Q(T)-\gamma Q(T)^2,\\
\frac{\mathrm{d}M}{\mathrm{d}T} &= \frac{1}{\omega}\left(P(T)-M(T)\right).
\end{aligned} \tag{2.1}$$

with initial conditions

$$P_0 = P(T)\geq 0,\ Q_0 = Q(T)\geq 0,\ M_0 = M(T)\geq 0.$$

Here parameter α is the strength of growth rate of prey, K stands for the carrying capacity for prey species and κ is for the survival threshold for a strong Allee effect. Besides, μ represents the consumption ratio or predator capture rate of the prey, β is the constant for half saturation and ν in the second equation for predator represents the conversion efficacy of prey species to predator species. The parameter η is associated with natural death of predator species and parameter γ is the strength of intraspecific competition.

Now we demonstrate how to derive the last equation in the system of (2.1), providing a memory contribution in the system. Since the density of predator is associated with past and present density of prey species, a nonlocal term can be considered with a continuous density function, represented with $\mathscr{A}$ [5]. This function has a task by weighting past moments in the system. Therefore, the prey density in the second equation of system (2.1) can be substituted with the expression

$$M(T) = \int_{-\infty}^{T} P(s)\mathscr{A}(T-s)\mathrm{d}s, \tag{2.2}$$

with a probability density presented by $\mathscr{A}(t) = exp(-t/\omega)/\omega$, satisfying

$$\int_{0}^{\infty} \mathscr{A}(t)\mathrm{d}t = 1, \quad \text{with} \quad \mathscr{A} : [0,\infty) \to \mathbb{R}.$$

Note that ω measures the past influence. Here, smaller $1/\omega$ (larger ω) implies the existence of past influence for larger time interval. For details of this approach, we refer the reader to papers [5, 13, 14]. Differentiating the statement given by Eq. (2.2), one obtains the last differential equation in the system of Eq. (2.1).

2.1. Dimensionless model

To reduce the number of parameters, new dimensionless variables can be introduced as $P = K\tilde{P}, \quad Q = K^2\alpha\tilde{Q}/\mu, \quad M = K\tilde{M}, \quad t = \tilde{t}/K\alpha$, and new parameters as

$$\tilde{\kappa} = \frac{\kappa}{K}, \quad \tilde{\beta} = \frac{\beta}{K^2}, \quad \tilde{\nu} = \frac{\nu\mu}{\alpha K}, \tilde{\eta} = \frac{\eta}{\alpha K}, \quad \tilde{\gamma} = \frac{\gamma K}{\alpha}, \quad \tilde{\omega}' = \frac{1}{\omega\alpha K},$$

the nondimensional model can be expressed by

$$\begin{aligned}
\frac{\mathrm{d}P}{\mathrm{d}T} &= P(T)(1-P(T))(P(T)-\kappa)-\frac{P(T)^2 Q(T)}{\beta+P(T)^2},\\
\frac{\mathrm{d}Q}{\mathrm{d}T} &= \frac{\nu M(T)^2 Q(T)}{\beta+M(T)^2}-\eta Q(T)-\gamma Q(T)^2,\\
\frac{\mathrm{d}M}{\mathrm{d}T} &= \omega'\left(P(T)-M(T)\right),
\end{aligned} \tag{2.3}$$

with non-negative initial conditions

$$P_0 = P(T)\geq 0,\ Q_0 = Q(T)\geq 0,\ M_0 = M(T)\geq 0.$$

2.2. Steady States

Depending on the parameter space, the model has four possible equilibria : one extinction, two predator free and one coexistence state:

- The extinction steady state $S_{000} = (0,0,0)$ is trivial and thus always exists in the system.
- There exist two predator free states that are given by $S_{101} = (P_s, 0, M_s)$ and $S'_{101} = (P'_s, 0, M'_s)$. Here, considering $Q = 0$ in Eq. (2.3) leads to $P^2-(\kappa+1)P+\kappa$ and thus $P_* = \{\kappa, 1\}$ and $M_* = P_*$.
- There exists one positive non-zero state $S_{111} = (P^s, Q^s, M^s)$ that has the relation

  $$(1-P)(P-\kappa)-\frac{PQ}{\beta_1+P^2} = 0.$$

  Here Q^s and M^s can be written in terms of P^s as

  $$Q^s = \frac{[(1-P^s)(P^s-\kappa)](\beta+P^{s2})}{P^s} \quad \text{and} \quad M^s = P^s.$$

3. Local Stability Analysis

The local stability for the system (2.3)-(2.3) can be performed through linearisation argument around a steady state $S=(P^s,Q^s,M^s)$, that is

$$\begin{aligned} P =&P^s+\bar{P}, \\ Q =&Q^s+\bar{Q}, \\ M =&M^s+\bar{M}, \end{aligned} \tag{3.1}$$

leading to a Jacobian matrix $D=(d_{ij}),\ i,j=\{1,2,3\}$ for which

$$\frac{\mathrm{d}}{\mathrm{d}t}\begin{bmatrix} P \\ Q \\ M \end{bmatrix} = \begin{bmatrix} d_{11} & d_{12} & d_{13} \\ d_{21} & d_{22} & d_{23} \\ d_{31} & d_{23} & d_{33} \end{bmatrix}\Bigg|_S \begin{bmatrix} \bar{P} \\ \bar{Q} \\ \bar{M} \end{bmatrix}, \tag{3.2}$$

where $\bar{}$ stands for the perturbed states and components of D matrix are given as

$$\begin{aligned} d_{11} =&\kappa(2P-1)+(2-3P)P-\frac{2\beta PQ}{(\beta+P^2)^2} \quad d_{12}=-\frac{P^2}{\beta+P^2}, \quad d_{13}=0, \quad d_{21}=0, \\ d_{22} =&\frac{\nu M^2}{\beta+M^2}-\eta-2\gamma Q, \quad d_{23}=\frac{2\beta_2\nu MQ}{(\beta+M^2)^2}, \quad d_{31}=\omega', \quad d_{32}=0, \quad d_{33}=-\omega'. \end{aligned}$$

3.1. Stability of S_{000} state

The characteristic polynomial corresponding the trivial extinction state $S_{000}=(0,0,0)$ is found by Det $\left[\varphi I_3-D|_{S_{000}}\right]=0$, leading to

$$(\varphi+\kappa)(\varphi+\eta)\left(\varphi+\omega'\right)=0, \tag{3.3}$$

for which I_3 represents a 3×3 identity matrix. Here all roots of Eq. (3.3) is found to be negative and thus trivial extinction state is always a stable node.

3.2. Stability of S_{101} and S'_{101} states

As stated in Sec. 2.2, there are two predator free axial states given by $S_{101}=(P_s,0,M_s)$ and $S'_{101}=(P'_s,0,M'_s)$. The roots of the characteristic polynomial corresponding to these steady states is found using

$$(\varphi-\kappa(2P_*-1)-(2-3P_*)P_*)\left(\varphi+\omega'\right)\left(\varphi-\frac{\nu M_*^2}{\beta+M_*^2}+\eta\right). \tag{3.4}$$

Thus eigenvalues are obtained as

$$\begin{aligned} \varphi_1 =&\kappa(2P_s-1)+(2-3P_s)P_s, \\ \varphi_2 =&-\omega', \\ \varphi_3 =&\frac{\nu {M_s}^2}{\beta+{M_s}^2}-\eta, \end{aligned}$$

Therefore the roots of this polynomial is found to be negative or have negative real part satisfying the conditions

$$\kappa(2P_s-1)+(2-3P_s)P_s<0 \quad \text{and} \quad \frac{\nu {M_s}^2}{\beta+{M_s}^2}<\eta.$$

3.3. Stability of S_{111} state

The characteristic equation at the positive coexisting state $S_{111}=(P^s,Q^s,M^s)$ can be computed using Det $\left[\varphi I_3-D|_{S_{111}}\right]=0$, leading to

$$(\varphi-d_{11})(\varphi-d_{22})(\varphi-d_{33})-d_{12}d_{23}d_{31}=0. \tag{3.5}$$

Therefore the local stability for the positive steady state can be determined solving Eq. (3.5).

In Fig. 3.1, the temporal dynamics the prey and predator densities and their corresponding phase diagram are demonstrated with respect to various values of memory rate ω'. Fig. 3.1(a,c,e), the dynamics of both species exhibit periodic oscillations, thus leading to unstable behaviour. The frequency of oscillations in Fig. 3.1(a) is larger compared with the frequency of oscillations in Fig. 3.1(c), where the rate of memory is increased from $\omega'=0.1$ to $\omega'=0.3$. Other parameters are $\kappa=0.1$, $\beta=0.5$, $\nu=1.8$, $\eta=0.7$ and $\gamma=0.4$. In both Fig. 3.1(a) and Fig. 3.1(c), the simulations are initiated using the coexisting state obtained with these parameters. Hence the dynamics stays at their equilibrium for about $t=500$ before oscillating. This can be more evident from Fig. 3.1(e), that the systems stays at the steady state for a longer time, e.g. till $t\in[0\ \ 1300]$, when increasing the memory rate from $\omega'=0.3$ to $\omega'=0.4$. Lastly, in 3.1(g), the system appears to be stable, yet it may be unstable at very large times. The corresponding phase diagrams for all these four cases are presented in 3.1(b,d,f,h), where the initial point of the trajectory is given by a yellow diamond sign; and end point of the trajectory is given by a magenta diamond sign.

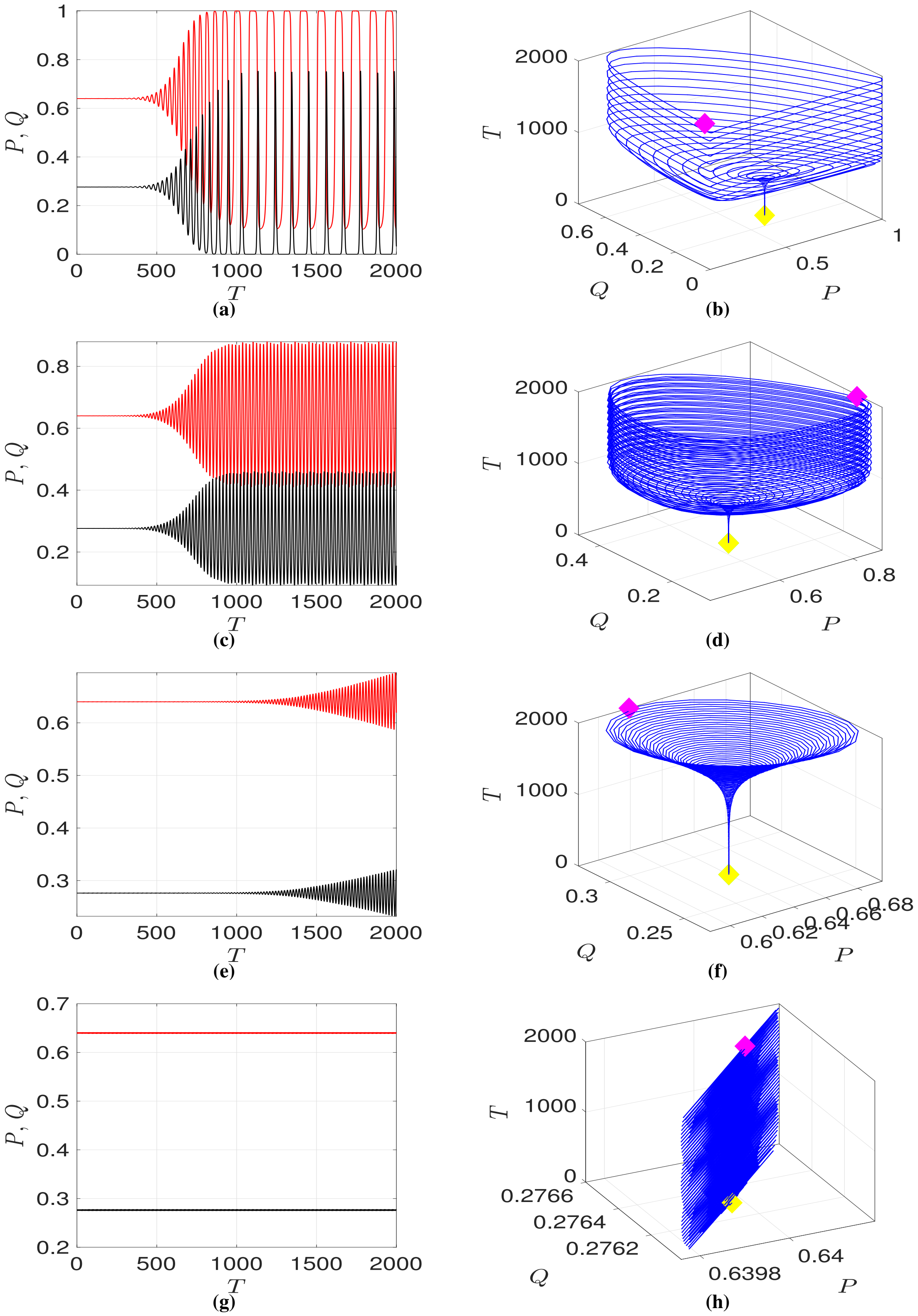

Figure 3.1: Densities of prey (P) and predator (Q) species with various memory rate, where $\omega' = 0.1$ (a), $\omega' = 0.3$ (c), $\omega' = 0.4$ (e) and $\omega' = 0.5$ (g). The red and black lines respectively stand for prey and predator species. The corresponding phase portraits are respectively given in (b,d,f,h). The initial and end points of the phase trajectories are given by yellow and magenta diamonds. Other parameters are $\kappa = 0.1$, $\beta = 0.5$, $\nu = 1.8$, $\eta = 0.7$ and $\gamma = 0.4$. The initial condition is given by the steady state corresponding to these parameters.

Figure 3.2 demonstrates dynamics of prey and predator for two different memory rate a smaller intraspecific competition strength, compared with Fig. 3.1. As seen a small decrease in the intraspecific competition may lead to extinction of both species, where parameter γ is reduced from $\gamma = 0.4$ to $\gamma = 0.38$. Increasing memory rate from $\omega' = 0.1$ to $\omega' = 0.4$, unstable dynamics with periodic oscillations appears again. Other parameter are same as Fig. 3.2.

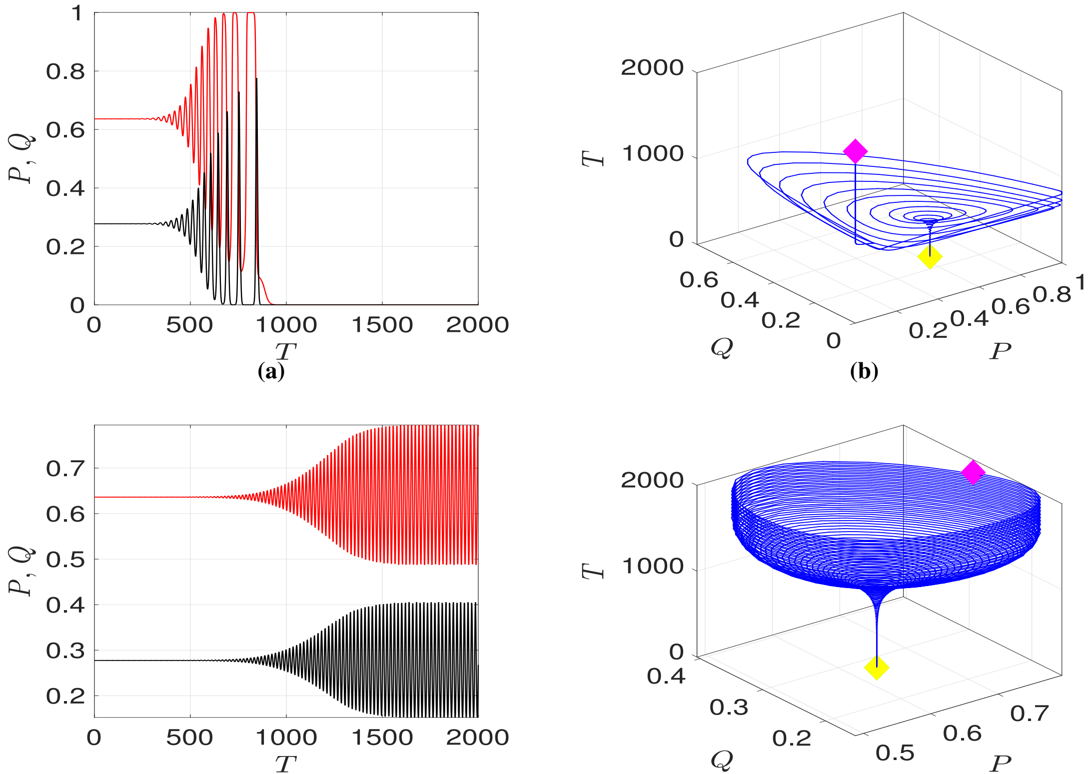

(a) **(b)**

(c) **(d)**

Figure 3.2: Densities of prey (P) and predator (Q) species with memory rates $\omega' = 0.1$ (a) and $\omega' = 0.4$ (c) for a smaller intraspecific competition $\gamma = 0.38$ (compared to Fig. 3.1). The red and black lines respectively stand for prey and predator species. The corresponding phase portraits are respectively given in (b,d). The initial and end points of the phase trajectories are given by yellow and magenta diamonds. Other parameters are $\kappa = 0.1$, $\beta = 0.5$, $\nu = 1.8$, $\eta = 0.7$. The initial condition is given by the steady state corresponding to these parameters.

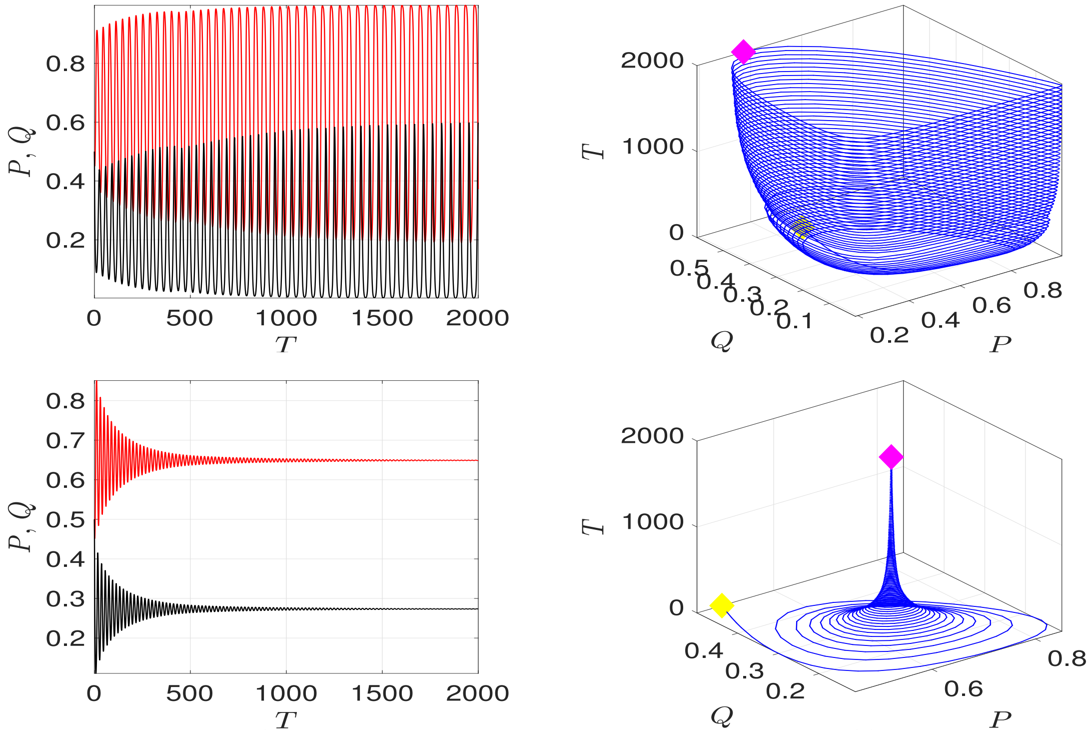

(c) **(d)**

Figure 3.3: Time evolutions of prey (P) and predator (Q) species with memory rates $\omega' = 0.1$ (a) and $\omega' = 0.38$ (c) for a larger intraspecific competition $\gamma = 0.45$ (compared to Fig. 3.1). The red and black lines respectively stand for prey and predator species. The corresponding phase portraits are respectively given in (b,d). The initial and end points of the phase trajectories are given by yellow and magenta diamonds. Other parameters are $\kappa = 0.1$, $\beta = 0.5$, $\nu = 1.8$, $\eta = 0.7$. The initial condition is chosen as $(P_0, Q_0, M_0) = (0.5, 0.5, 0.5)$.

Compared to Fig. 3.1, the role of a larger intraspecific competition ($\gamma = 0.45$) is presented in Fig. 3.3. As seen, smaller memory rate $\omega' = 0.1$ lead to an unstable system. However, increasing memory rate to $\omega' = 0.38$, the system stability is changed from unstable to stable. The initial conditions of the system is now chosen as $(P_0, Q_0, M_0) = (0.5, 0.5, 0.5)$. Figure 3.4 shows bifurcation diagrams and the existence of Hopf bifurcation occuring with respect to memory rate ω' for various intraspecific competition rates. Here it is chosen as $\gamma = 0.15$ (a), $\gamma = 0.2$ (b), $\gamma = 0.38$ (c) and $\gamma = 0.49$ (d), respectively. Here, the green and magenta circles represent the maximum and minimum points of the prey and predator dynamics at each memory rate. As seen in Fig. 3.4(a), for $\gamma = 0.2$, both prey and predator dynamics are always unstable for $\omega' \in [0, 1]$ regardless of the memory rate. In Fig. 3.4(b), a small region, e.g. $\omega' \in [0.9, 1]$, system becomes stable, yet unstable dynamics with periodic oscillations can be seen for smaller memory constant. Increasing intraspecific competition to $\gamma = 0.38$, the stable region is obtain for a larger interval of ω' and unstable dynamics are obtained for small values of memory rate. Lastly, in Fig. 3.4(d), for both very small and large values of memory rate ω', stable dynamics is observed. Only in a small region with $\omega' \in [0.09, 0.23]$, unstable dynamics where oscillations with small amplitude are obtained.

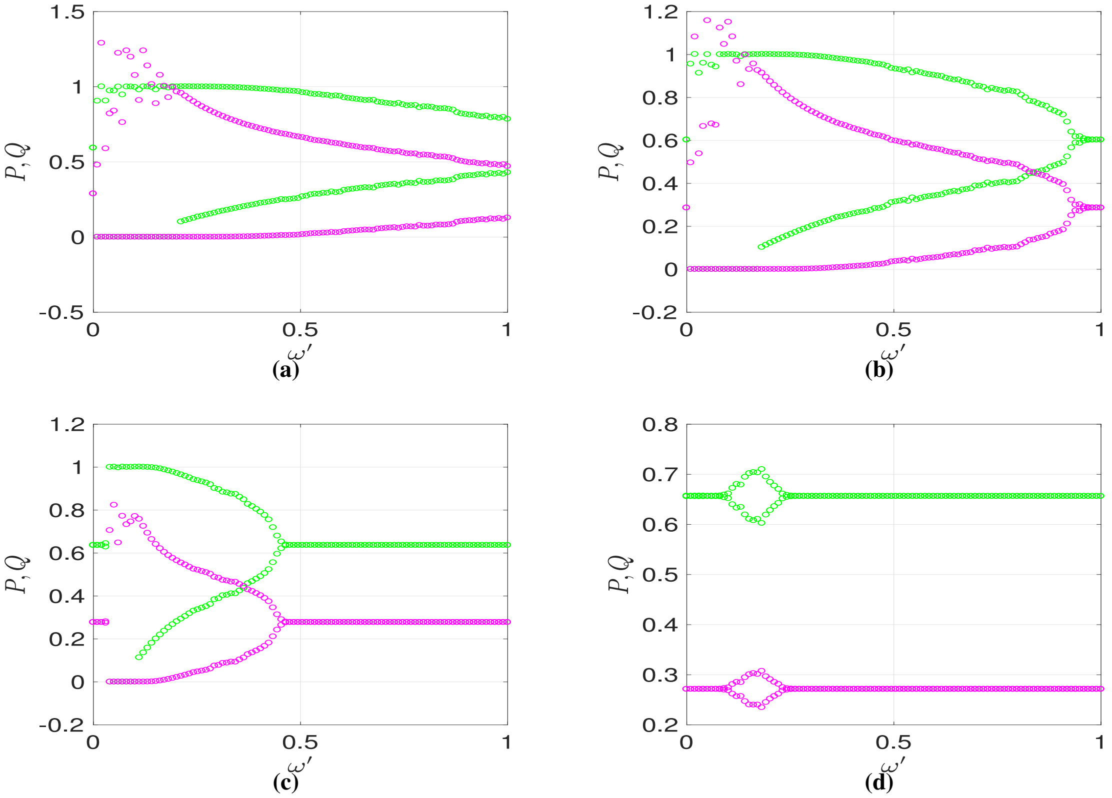

(a) **(b)**

(c) **(d)**

Figure 3.4: Densities of prey (P) and predator (Q) populations as a function of memory rate ω' for various intraspecific competition rates, where $\gamma = 0.15$ (a), $\gamma = 0.2$ (b), $\gamma = 0.38$ (c) and $\gamma = 0.49$. The green and magenta circles respectively stand for the dynamics of prey and predator species. The corresponding phase portraits are respectively given in (b,d). Other parameters are $\kappa = 0.1$, $\beta = 0.5$, $\nu = 1.8$, $\eta = 0.7$. The initial condition is chosen as $(P_0, Q_0, M_0) = (0.5, 0.5, 0.5)$.

Simulations presented in this section demonstrate that larger values of ω' has a stabilising role in the dynamics of both prey and predator populations. This also implies that smaller values of ω' account for the past influence for a larger time interval. The intraspecific competition parameter γ has also a significant impact on the dynamics, where depending on the memory parameter ω', the change in γ may induce extinction, stability or instability of species densities.

4. Summary

In prey predator interactions, predator population may expose to Allee effect, and this leads to an influence on the survival probability of each individual. The existence of Allee effect has been experimentally demonstrated in various species, including for example mammals such as suricates [15], and marine invertebrates such as gastropod [16]. Furthermore infraspecific competition is known to exist among species and occurs very common in nature due to limited sources and difficulties in mate finding. Therefore the inclusion of memory term in a model with Allee effect and intraspecific competition provide an additional degree of realism.

In this paper, a mathematical system comprising Allee effect with fading memory is considered. In fact, the fading memory is crucial in real prey-predator dynamics in ecology as the density of predator is highly dependent not only on the density of prey at the present time but also on the density of prey in the past. In our model, we also consider intraspecific competition as an additional degree of realism in the mathematical modeling. In this paper, we concentrate on the role of memory rate ω' and intraspecific competition γ [5, 17]. Besides, Holling type III functional response, that assumes that the predator species effectively seeks for prey species, is considered. The most important finding of this paper is the dramatic change in the dynamics with ω' and γ. In this context, for a fixed memory rate, larger intraspecific competition lead to stability of the system. Furthermore, the memory rate ω' refers to the measure of the past influence. Namely, larger ω' stands for the past effect for a larger time interval. The system tends to be unstable with larger ω'.

This work can be extended in a couple of direction. The more straightforward extension would be to inclusion of local and non-local delay terms, as switching from one state to another state is not immediate and require some time delay [18]. This could be in the growth rate of prey or in the maturation of predator. Besides, the random fluctuations may occur in nature as a result of climate change or other factors including some short term diseases. Thus another extension would be to consider environmental noise terms in the parameters of the model to capture more realistic dynamics of prey-predator model investigated here [19, 20]. Furthermore, wide spectrum of numerical techniques can be applied to approximate the solutions of the model [21, 22]. The local stability analysis of the system is extensively studied. Following the ideas in [23], the global stability of the model can be analysed through LaSalle's Invariance Principle-Lyapunov's direct method.

Acknowledgements

The authors would like to express their sincere thanks to the editor and the anonymous reviewers for their helpful comments and suggestions.

Funding

There is no funding for this work.

Availability of data and materials

Not applicable.

Competing interests

The authors declare that they have no competing interests.

Author's contributions

The authors constructed and analysed the model and performed the numerical simulations, the authors has also written the original manuscript and gave final approval of the current version and any revised version to be submitted to the journal. All authors contributed equally to the writing of this paper. All authors read and approved the final manuscript.

References

[1] A. J. Lotka, *Elements of physical biology*, Science Progress in the Twentieth Century, **21**(82) (1926), 341-343.
[2] V. Volterra, *Fluctuations in the abundance of a species considered mathematically*, Nature, **119**(2983), 12-13.
[3] E. Renshaw, *Modelling Biological Populations in Space and Time*, No. 11, Cambridge University Press, 1993.
[4] C. S. Holling, *Some characteristics of simple types of predation and parasitism*, Can. Entomol., **91**(7) (1959), 385-398.
[5] B. Sahoo, S. Poria, *Dynamics of predator–prey system with fading memory*, Appl. Math. Comput., 347 (2019), 319-333.
[6] S. Djilali, B. Ghanbari, *Dynamical behavior of two predators–one prey model with generalized functional response and time-fractional derivative*, Adv. Differ. Equ., **2021**(1) (2021), 1-19.
[7] B. Sahoo, B, *A predator-prey model with general holling interactions in presence of additional food*, Int. J. Plant Res., **2**(1) (2012), 47-50.
[8] W. C. Allee, *Animal aggregations*, Q. Rev. Biol., **2**(3) (1927), 367-398.
[9] P. C. Tabares, J. D. Ferreira, V. Rao, *Weak Allee effect in a predator-prey system involving distributed delays*, Comput. Appl. Math., **30**(3) (2011), 675-699.
[10] Y. Song, S., Wu, H. Wang, *Spatiotemporal dynamics in the single population model with memory-based diffusion and nonlocal effect*, J. Differ. Equ., **267**(11) (2019), 6316-6351.
[11] Z. Ma, *Hopf bifurcation of a generalized delay-induced predator–prey system with habitat complexity*, Int. J. Bifurc. Chaos., **30**(06) (2020), 2050082.
[12] P. Shome, A., Maiti, A., S. Poria, *Effects of intraspecific competition of prey in the dynamics of a food chain model*, Model. Earth Syst. Environ., **2**(4) (2016), 1-11.
[13] M. Cavani, M. Farkas, *Bifurcations in a predator-prey model with memory and diffusion. I: Andronov-Hopf bifurcation*, Acta Math. Hungarica, **63**(3) (1994), 213-229.
[14] U. Ghosh, S. Pal, M. Banerjee, *Memory effect on Bazykin's prey-predator model: Stability and bifurcation analysis*, Chaos Solit. Fractals, 143 (2021), 110531.
[15] F. Courchamp, B. Grenfell, T. Clutton-Brock, *Impact of natural enemies on obligately cooperative breeders*, Oikos **91**(2) (2000), 311-322.
[16] A. W. Stoner, M. Ray-Culp, *Evidence for allee effects in an over-harvested marine gastropod: density-dependent mating and egg production*, Mar. Ecol. Prog. Ser. **202** (2000), 297-302.
[17] J. D. Ferreira, C. A. T. Salazar, P. C. Tabares, *Weak Allee effect in a predator–prey model involving memory with a hump*, Nonlinear Anal. Real World Appl., **14**(1) (2013) 536-548.
[18] A. Gökçe, *Numerical bifurcation analysis for a prey-predator type interactions with a time lag and habitat complexity*, Bitlis Eren Üni. Fen Bilimleri D., **10**(1) (2020), 57-66.
[19] A. Gökçe, *A mathematical modeling approach to analyse the effect of additional food in a predator-prey interactions with a white Gaussian noise in Prey's growth rate*, Int. J. Appl. Comput., **8**(1) (2022), 1-20.
[20] A. Gökçe, *Exploring a simple stochastic mathematical model including fear with a linear functional response*, Fundam. J. of Math. and Appl., **4**(4) (2021), 280-288.
[21] B. Gürbüz, *A numerical scheme for the solution of neutral integro-differential equations including variable delay*, Math. Sci., (2021), 1-9.
[22] B. Gürbüz, *Laguerre matrix-collocation technique to solve systems of functional differential equations with variable delays*, AIP Conf. Proc., AIP Publishing LLC, (2019), 090007.
[23] S. Çakan, *Dynamic analysis of a mathematical model with health care capacity for COVID-19 pandemic*, Chaos Solit. Fractals, **139** (2020), 110033.